Research Square

Preprints are preliminary reports that have not undergone peer review.
They should not be considered conclusive, used to inform clinical practice,
or referenced by the media as validated information.

Receiver Sensitivity Limits, Forward Error Correction, and Adaptive Beam Divergence for Space Laser Links: When Does Adapting the Beam Pay Off?

SATHISHA R N

sathisharyan@sit.ac.in

Siddaganga Institute of Technology https://orcid.org/0000-0001-8031-7611

Research Article

Keywords: free-space optical communication, inter-satellite links, receiver sensitivity, quantum limit, forward error correction, low-density parity-check, pointing jitter, adaptive divergence, liquid lens, outage probability

Posted Date: November 17th, 2026

DOI: https://doi.org/10.21203/rs.3.rs-11706630/v2

License: This work is licensed under a Creative Commons Attribution 4.0 International License.
Read Full License

Additional Declarations: The authors declare no competing interests.

Receiver Sensitivity Limits and Adaptive Beam Divergence for Space Laser Links: When Does Adapting the Beam Pay Off?

Sathisha R. N., *Member, IEEE*

***Abstract*—Space laser terminals for low-Earth-orbit (LEO) to geostationary (GEO) data relay must close links near -55 dBm while the platform jitters by a few microradians. We first compare four 1550 nm receivers (PIN, avalanche photodiode, optically pre-amplified on-off keying, and pre-amplified differential phase-shift keying (DPSK)) against the binary-DPSK quantum limit, with and without 7% hard-decision forward error correction (FEC). Pre-amplified DPSK meets -55 dBm at a bit error rate of 10^{-6} only up to 595 Mb/s, and up to 1.5 Gb/s with FEC. At 10 Gb/s, -55 dBm provides 2.47 photons/bit, below the 5.2 photons per information bit that even an ideal binary DPSK receiver with this FEC requires. A flat power specification across rates is therefore unachievable for binary formats. We then study transmit divergence under Rayleigh-distributed pointing jitter. For a fixed-rate link, the outage-optimal divergence places the peak received power at e times the receiver sensitivity, independent of the jitter level; we prove this and confirm it by Monte Carlo simulation. For a rate-adaptive link, the divergence that maximizes the rate guaranteed at a given outage scales linearly with jitter, which recovers the classical minimum-power design. Gamma-gamma turbulence makes the fixed-rate optimum jitter-dependent again. A 60 s time-domain simulation of a LEO–GEO terminal with a four-state liquid lens shows a 95% throughput gain over the best fixed beam during platform disturbances, and an advantage that persists for actuation latencies up to 0.5 s. Adaptive divergence therefore pays off for rate-adaptive terminals and for links through the atmosphere, but not for fixed-rate inter-satellite links.**

***Index Terms*—Free-space optical communication, inter-satellite links, receiver sensitivity, quantum limit, DPSK, pointing jitter, beam divergence, liquid lens, outage probability.**

I. Introduction

LASER inter-satellite links are operational. The European Data Relay System relays LEO data through GEO at 1.8 Gb/s over link distances near 45,000 km [1]. Surveys identify receiver sensitivity and pointing as the two dominant design constraints of such links [2]. Two questions follow for any new relay terminal: how sensitive must the receiver be, and how wide should the transmitted beam be when the platform jitters?

Receiver requirements are often written as a single power level over a range of data rates. A 2025 research call from the Indian Space Research Organisation, for example, asks for a 1550 nm receiver that operates below -55 dBm from 50 Mb/s to 10 Gb/s at a bit error rate (BER) near 10^{-6} [3]. Photon-efficient receiver design shows that the meaningful figure is photons per bit, which a fixed power level cannot hold constant across rates [4].

Beam divergence trades on-axis gain against tolerance to pointing error. Chen and Gardner showed that an optimal transmit gain minimizes the power needed under random pointing error [5], and Arnon *et al.* optimized the transmitter aperture under pointing vibration [6]. Toyoshima *et al.* derived the divergence-to-jitter ratio that minimizes the average BER [7]. Farid and Hranilovic optimized beam width for outage capacity with pointing errors and turbulence [8], Arnon *et al.* analyzed vibration and turbulence together for downlinks [9], and Xue *et al.* maximized link reliability through divergence selection [10]. Adaptive beam width under vibration was proposed by Arnon [11]. Variable-focus (liquid) lenses now make adaptive divergence possible without moving parts: they have been demonstrated on a 10 Gb/s, 104 m link [12] and proposed for dynamic beam control on inter-satellite links [13], and commercial devices have passed initial environmental tests for space use [14]. A beam-divergence control system for small space terminals has also been prototyped and validated, covering 90–6,250 μrad [15]. In our earlier work, focus-tunable liquid lenses set the divergence, and hence the link length or cell coverage, of indoor laser-based optical wireless links [16]–[18]; here we ask when such control is worth having in space.

What remains unclear is *when* adapting the divergence is worth its cost. The answer depends on the performance metric and on the operating mode of the link. Average-BER optimization [7] suits jitter that is fast relative to a codeword. Platform disturbances such as reaction-wheel crossings and thruster firings are slow, so outage is the relevant metric, and it behaves differently. This paper makes four contributions:

1) A comparison of four 1550 nm receivers referenced to the binary-DPSK quantum limit, with and without 7% hard-decision FEC, quantifying the rates at which a -55 dBm requirement can be met.
2) A closed-form proof, confirmed by Monte Carlo simulation, that for a fixed-rate link under Rayleigh pointing jitter the outage-optimal divergence is independent of the jitter level and places the peak received power at e times the sensitivity. This is consistent with the reliability analysis of [10], and we state it explicitly as a design rule.
3) The contrasting rate-adaptive result, in which the optimal

The author is with the Department of Electronics and Telecommunication Engineering, Siddaganga Institute of Technology, Tumakuru 572103, Karnataka, India (e-mail: sathisharn@sit.ac.in; satisharyan@gmail.com). ORCID: 0000-0001-8031-7611.

divergence scales linearly with jitter and coincides with the minimum-power design of [5], and a Monte Carlo study showing that gamma-gamma turbulence makes the fixed-rate optimum jitter-dependent again.

4) A 60 s time-domain simulation of a LEO–GEO terminal with a four-state liquid-lens controller, including the effect of actuation latency.

Section II gives the system model. Section III treats receiver limits, Section IV the divergence optimization, and Section V the liquid-lens terminal. Section VI discusses design implications and limitations, and Section VII concludes.

II. System Model

A. Receivers

All receivers operate at $\lambda = 1550$ nm with quantum efficiency 0.8, giving a responsivity $\mathcal{R} \approx 1.0$ A/W. For on-off keying (OOK) we use the Gaussian approximation

$$\mathrm{BER} = \tfrac{1}{2}\,\mathrm{erfc}\!\left(\frac{Q}{\sqrt{2}}\right), \qquad Q = \frac{I_1 - I_0}{\sigma_1 + \sigma_0}, \tag{1}$$

where $I_{1,0}$ are the photocurrents of the two symbols and $\sigma_{1,0}$ the corresponding noise standard deviations. Table I lists all parameters.

PIN: shot, dark-current and thermal noise. The transimpedance amplifier is matched to the bit rate, $R_L = 1/(2\pi C_T B_e)$ with $B_e = 0.7R_b$, so thermal noise grows as B_e^2.

Avalanche photodiode (APD): excess noise factor $F(M) = k_A M + (1 - k_A)(2 - 1/M)$ [19]; the gain M is optimized at every operating point.

Pre-amplified OOK: an erbium-doped fiber amplifier (EDFA) of gain G precedes a PIN detector. With amplified spontaneous emission (ASE) density $S_{sp} = n_{sp} h\nu (G-1)$ per polarization, the beat-noise variances for input power P are [20]

$$\sigma^2_{s\text{-}sp} = 4\mathcal{R}^2 G P S_{sp} B_e, \qquad \sigma^2_{sp\text{-}sp} = 2\mathcal{R}^2 S^2_{sp}(2B_o - B_e)B_e, \tag{2}$$

with both ASE polarizations, an optical filter of bandwidth B_o, and a free-space-to-fiber coupling loss ahead of the amplifier.

Pre-amplified DPSK: balanced detection after a one-bit delay-line interferometer. With N_p photons per bit entering the amplifier,

$$\mathrm{BER}_{\mathrm{DPSK}} = \tfrac{1}{2}\exp(-\eta_{\mathrm{pen}} N_p / n_{sp}), \tag{3}$$

where η_{pen} is an implementation penalty. For an ideal amplifier ($n_{sp} = 1$, no penalty) this reduces to $\frac{1}{2}e^{-N_p}$, the binary-DPSK quantum limit: 13.1 photons/bit at BER 10^{-6} [4].

B. Forward Error Correction

We add a 7%-overhead hard-decision FEC with a pre-FEC BER threshold of 3.8×10^{-3}, typical of the enhanced codes in [21]. The receiver then operates at line rate $1.07R_b$ and target BER 3.8×10^{-3}; sensitivity is quoted per information bit.

TABLE I
Simulation Parameters

Parameter	Value
Wavelength; quantum efficiency	1550 nm; 0.8
Dark current; temperature	5 nA; 300 K
TIA capacitance; noise factor	0.3 pF; 3 dB
Electrical bandwidth	$0.7R_b$
APD ionization ratio k_A; max gain	0.45; 40
EDFA gain; noise figure	30 dB; 4.5 dB
Optical filter B_o	12.5 GHz (0.1 nm)
Free-space-to-fiber coupling loss	2 dB
DPSK implementation penalty	1.5 dB
OOK extinction ratio	15 dB
Target BER (uncoded)	10^{-6}
HD-FEC overhead; pre-FEC threshold	7%; 3.8×10^{-3}
Transmit power; optics loss (Tx, Rx)	1 W; 3 dB, 3 dB
LEO–GEO distance; receive aperture	40,000 km; 0.20 m

C. Link and Pointing

A Gaussian beam with $1/e^2$ half-angle divergence θ delivers a peak received power $P_{pk}(\theta) = K/\theta^2$, where K collects the transmit power, receive aperture area, link distance and optics losses (equivalent transmit gain $8/\theta^2$). A radial pointing error θ_e reduces the received power to

$$P_{rx} = \frac{K}{\theta^2}\exp\!\left(-\frac{2\theta_e^2}{\theta^2}\right). \tag{4}$$

Azimuth and elevation errors are independent, zero-mean Gaussian, each with standard deviation σ, so θ_e is Rayleigh distributed and θ_e^2 is exponential with mean $2\sigma^2$. Spacecraft microvibrations relevant to laser terminals have been measured in orbit [22]. In Section V the jitter on each axis is a first-order autoregressive process with 50 Hz bandwidth: slow relative to a bit and comparable to a codeword, so outage is the relevant metric.

D. Turbulence

For LEO-to-ground downlinks the irradiance is scaled by a unit-mean gamma-gamma variable [23], with parameters α, β set by the Rytov variance σ_R^2 (plane wave, zero inner scale). We use $\sigma_R^2 = 0.2$, 1 and 3, and combine turbulence and pointing by Monte Carlo simulation with 2×10^5 samples per point.

III. Receiver Sensitivity Limits

Table II and Fig. 1 give the sensitivities. Pre-amplified DPSK needs a constant 41 photons/bit, 5 dB above the quantum limit: 2 dB from coupling loss, 1.5 dB from the implementation penalty and 1.5 dB from $n_{sp} = 1.41$. With FEC this falls to 16.5 photons per information bit. Pre-amplified OOK needs 115 to 750 photons/bit; at low rates its fixed 12.5 GHz filter makes ASE–ASE beat noise dominant. The APD needs 572 to 1328 photons/bit, and the PIN about 6,900.

The last row of Table II answers the specification question. At 10 Gb/s, -55 dBm provides only 2.47 photons/bit, which is below both the uncoded binary-DPSK limit (13.1) and the limit with 7% HD-FEC (5.2 photons per information bit). Even

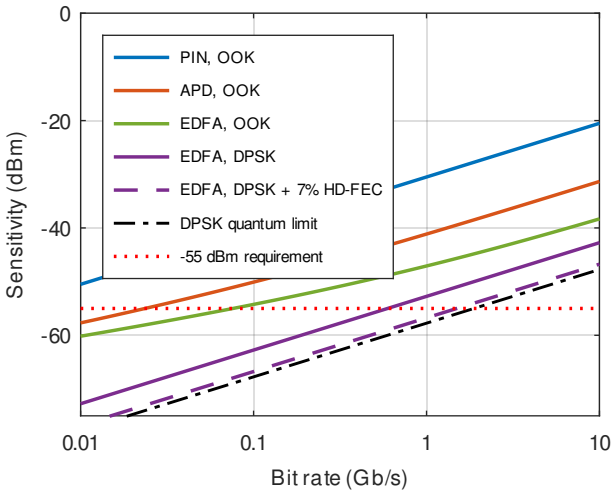

Fig. 1. Sensitivity at BER 10^{-6} versus bit rate. The FEC curve is per information bit. The dotted line marks a -55 dBm requirement.

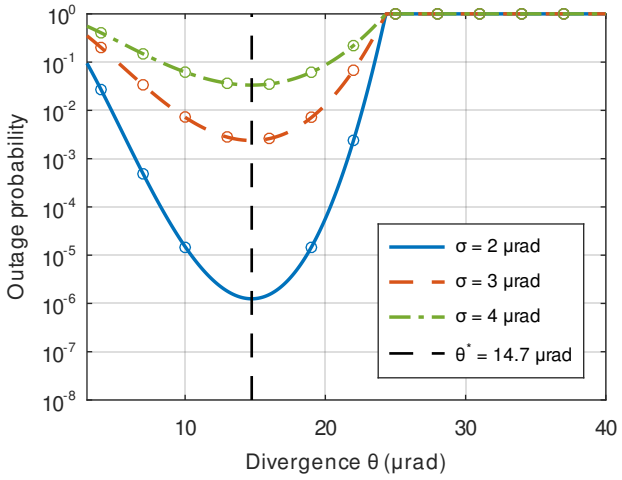

Fig. 2. Fixed-rate outage versus divergence, LEO–GEO link at 1 Gb/s. Lines: closed form (5). Circles: Monte Carlo (2×10^6 samples). The optimum θ^* is the same for every jitter level.

TABLE II
SENSITIVITY (DBM) AT BER 10^{-6}

Bit rate	PIN OOK	APD OOK	EDFA OOK	EDFA DPSK	DPSK +FEC	DPSK QL
50 Mb/s	−43.5	−52.5	−56.1	−65.8	−69.8	−70.8
100 Mb/s	−40.5	−50.1	−54.2	−62.7	−66.8	−67.7
250 Mb/s	−36.5	−46.7	−51.6	−58.8	−62.8	−63.8
500 Mb/s	−33.5	−44.0	−49.4	−55.8	−59.8	−60.8
1 Gb/s	−30.5	−41.1	−47.1	−52.7	−56.8	−57.7
2.5 Gb/s	−26.5	−37.3	−43.8	−48.8	−52.8	−53.8
5 Gb/s	−23.5	−34.3	−41.1	−45.8	−49.8	−50.8
10 Gb/s	−20.5	−31.3	−38.3	−42.7	−46.8	−47.7
Highest rate meeting −55 dBm:						
	–	24M	76M	595M	1.5G	1.88G

QL: uncoded binary-DPSK quantum limit (13.1 photons/bit).

TABLE III
LINK BUDGETS: RECEIVED POWER AND HIGHEST RATE (MB/S) AT BER 10^{-6} (CAPPED AT 10,000)

Link	L (km)	θ (μrad)	D_r (m)	P_{rx} (dBm)	APD OOK	EDFA OOK	EDFA DPSK
LEO–ground†	1,000	15	0.40	−13.5	10,000	10,000	10,000
LEO–LEO	4,000	15	0.10	−34.6	4,727	10,000	10,000
GEO–ground†	38,000	10	1.00	−33.6	5,920	10,000	10,000
LEO–GEO	40,000	10	0.20	−45.0	383	1,783	5,912

†Includes 3 dB atmospheric loss. No pointing loss.

an ideal binary DPSK receiver with this FEC meets -55 dBm only up to 4.7 Gb/s. Formats such as pulse-position modulation with photon counting can operate at fewer photons per bit [4], but they trade spectral efficiency and are a different design. For binary DPSK or OOK terminals, a requirement over 50 Mb/s–10 Gb/s should therefore be written as photons per bit or as sensitivity that scales with rate, for example -55 dBm at 500 Mb/s and -43 dBm at 10 Gb/s uncoded.

Table III applies these receivers to four links with 1 W transmit power. The LEO–GEO relay is the binding case: pre-amplified DPSK supports 5.9 Gb/s uncoded, and 10 Gb/s with FEC, before any pointing loss. This is consistent with the 1.8 Gb/s operational EDRS service [1], which carries margins for pointing, acquisition and ageing. Pointing loss on this link is the subject of Section IV.

IV. DIVERGENCE OPTIMIZATION UNDER POINTING JITTER

A. Fixed Rate: the Optimum Is Independent of Jitter

Proposition 1. *For a fixed-rate link with sensitivity S and the channel* (4) *with Rayleigh pointing error, the outage probability is*

$$P_{\text{out}}(\theta) = \exp\left[-\frac{\theta^2}{4\sigma^2}\ln\frac{K}{\theta^2 S}\right], \qquad \frac{K}{\theta^2} > S, \tag{5}$$

and $P_{\text{out}} = 1$ otherwise. It is minimized at

$$\theta^* = \sqrt{\frac{K}{eS}} \iff P_{pk}(\theta^*) = eS, \qquad P^*_{\text{out}} = \exp\left(-\frac{\theta^{*2}}{4\sigma^2}\right), \tag{6}$$

which does not depend on σ.

Proof. Outage occurs when $\theta_e^2 > (\theta^2/2)\ln(K/(\theta^2 S))$. Since θ_e^2 is exponential with mean $2\sigma^2$, (5) follows. With $u = \theta^2$, minimizing P_{out} is equivalent to maximizing $g(u) = u\ln(K/(uS))$, because σ only scales the exponent. Then $g'(u) = \ln(K/(uS)) - 1 = 0$ gives $u^* = K/(eS)$, and $g''(u) = -1/u < 0$ confirms a maximum. □

The outage-optimal beam is the one whose on-axis power exceeds the sensitivity by exactly e (4.34 dB), whatever the jitter. Jitter sets how low the best outage can be, not where it occurs. For the LEO–GEO link at 1 Gb/s ($S = -52.75$ dBm), $\theta^* = 14.75$ μrad. Fig. 2 plots (5) for $\sigma = 2$, 3 and 4 μrad together with Monte Carlo estimates from 2×10^6 samples; the curves agree, and the numerical minimum lies at 14.78 μrad for all three, within the grid step. The minimum outage rises from 1.25×10^{-6} to 3.34×10^{-2} as σ doubles from 2 to 4 μrad.

This result is consistent with the reliability-maximizing design of [10]. It differs from the average-BER optimum [7],

TABLE IV
RATE-ADAPTIVE LEO–GEO LINK, PRE-AMPLIFIED DPSK, $P_{\text{out}} = 10^{-3}$

σ (μrad)	θ_{opt} (μrad)	P_g (dBm)	Rate, adaptive (Mb/s)	Rate, $\theta = 5.26$ (Mb/s)
0.5	2.6	−37.8	10,000‡	10,000‡
1.0	5.3	−43.8	7,871	7,871
2.0	10.5	−49.8	1,968	392
3.0	15.8	−53.3	875	0
4.0	21.0	−55.8	492	0
5.0	26.3	−57.8	315	0

‡Capped at 10 Gb/s.

TABLE V
OUTAGE-OPTIMAL DIVERGENCE WITH GAMMA-GAMMA TURBULENCE, LEO–GROUND AT 10 GB/S (MONTE CARLO, 2×10^5 SAMPLES)

σ_R^2	θ_{opt} (μrad) / minimum P_{out} $\sigma = 1$ μrad	$\sigma = 3$ μrad
0 (jitter only)	27.6 / $\approx 10^{-83}$	27.6 / 6.4×10^{-10}
0.2	3.2–13.6 / $\leq 2.5 \times 10^{-6}$§	12.6 / 1.6×10^{-4}
1.0	3.4 / 7.0×10^{-5}	9.3 / 1.3×10^{-2}
3.0	3.2 / 2.4×10^{-3}	8.6 / 4.3×10^{-2}

§Below the Monte Carlo floor over this range.

whose fixed divergence-to-jitter ratio scales with σ. The two criteria apply to different jitter regimes: average BER to jitter that is fast relative to a codeword, outage to slow jitter.

B. Rate-Adaptive: the Optimum Scales With Jitter

A rate-adaptive terminal selects the highest rate whose sensitivity is met with probability $1-P_{\text{out}}$. The power guaranteed at that probability is

$$P_g(\theta) = \frac{K}{\theta^2} \exp\left(\frac{4\sigma^2 \ln P_{\text{out}}}{\theta^2}\right). \tag{7}$$

Maximizing over $u = \theta^2$ gives

$$\theta_{\text{opt}} = \sigma\sqrt{-4 \ln P_{\text{out}}}, \qquad P_g(\theta_{\text{opt}}) = \frac{K}{e\,\theta_{\text{opt}}^2}. \tag{8}$$

This is the minimum-transmit-power design of [5], read here as a rule for rate adaptation. For $P_{\text{out}} = 10^{-3}$, $\theta_{\text{opt}} = 5.26\sigma$. On the LEO–GEO link (Table IV, Fig. 3) the optimum doubles when the jitter doubles and the supported rate falls about fourfold. A beam fixed at the 1 μrad optimum loses the link once jitter exceeds 2.8 μrad, while the adapted beam degrades smoothly.

C. Turbulence Makes the Fixed-Rate Optimum Jitter-Dependent

For a LEO-to-ground downlink we take a small terminal: 1,200 km slant range, 0.2 W, 0.10 m receive aperture, 2 dB atmospheric loss, and 10 Gb/s DPSK ($S = -42.7$ dBm). Jitter alone would give $\theta^* = 27.6$ μrad at every σ. Scintillation adds fades that a narrower, stronger beam rides through, so the optimum shrinks and depends on jitter again (Table V, Fig. 4).

Turbulence moves the optimum two to nine times narrower than the jitter-only value, and at moderate turbulence ($\sigma_R^2 = 1$) tripling the jitter moves it from 3.4 to 9.3 μrad. For ground links, adaptive divergence is therefore useful even at a fixed rate, consistent with the downlink analysis of [9].

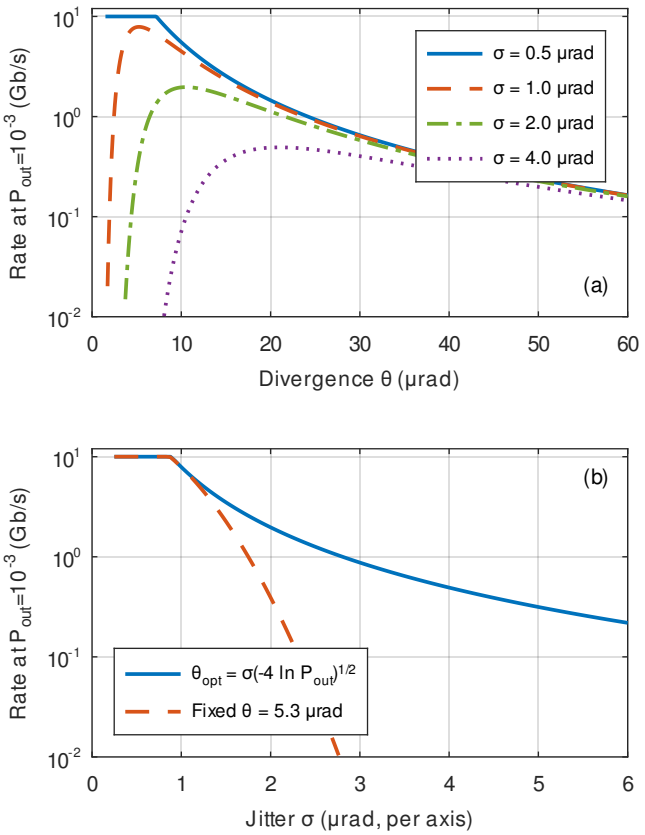

Fig. 3. Rate-adaptive LEO–GEO link at $P_{\text{out}} = 10^{-3}$. (a) Supported rate versus divergence for four jitter levels. (b) Adaptive divergence (8) versus a beam fixed at the 1 μrad optimum.

V. LIQUID-LENS ADAPTIVE TERMINAL

A. Scenario and Controller

We simulate 60 s of the LEO–GEO relay of Table I at 1 kHz. The per-axis jitter is 0.6 μrad when quiet and rises during three disturbances: a reaction-wheel speed crossing (10–20 s, 2.5 μrad), a thruster firing (30–34 s, 5.0 μrad) and an antenna slew (45–55 s, 1.5 μrad), with transitions smoothed over 0.2 s. The lens has four divergence states: 3, 6, 12 and 24 μrad.

Every 0.1 s the controller estimates σ from the tracking-sensor residual over the last 0.2 s, using $\mathrm{E}[\theta_e^2] = 2\sigma^2$, inflates the estimate by 1.2, and selects the state that maximizes P_g at $P_{\text{out}} = 10^{-3}$. It then sets the highest rate whose sensitivity P_g meets. Throughput counts only bits delivered while the instantaneous power meets that rate's sensitivity. Fixed beams use the same rate adaptation.

B. Results

Table VI confirms both regimes of Section IV. At a fixed 1 Gb/s, the best fixed beam is 12 μrad with 99.2% availability, close to the jitter-independent optimum of 14.75 μrad; a lens

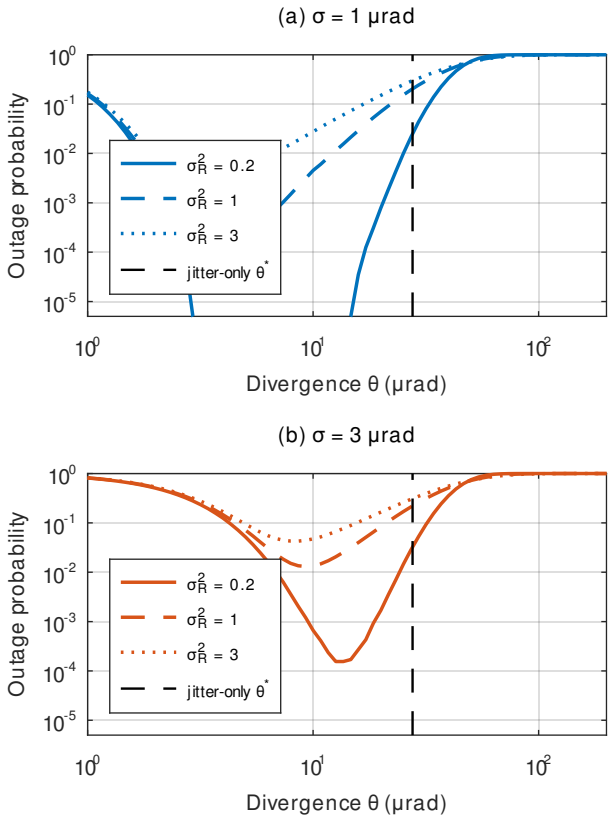

Fig. 4. Outage versus divergence with gamma-gamma turbulence and pointing jitter, LEO–ground at 10 Gb/s. (a) $\sigma = 1$ μrad. (b) $\sigma = 3$ μrad. Dashed vertical line: jitter-only optimum.

TABLE VI
FIXED BEAMS VERSUS ADAPTIVE LENS OVER THE 60 S EPISODE

Divergence	Avail. at	Throughput (Mb/s)		
	1 Gb/s	Quiet	Disturbed	Overall
Fixed 3 μrad	91.6%	9,717	67	5,832
Fixed 6 μrad	97.4%	9,842	694	6,160
Fixed 12 μrad	99.2%	3,685	1,264	2,710
Fixed 24 μrad	82.0%	996	680	869
Adaptive lens	–	9,850	1,357	6,431

adds little. With rate adaptation no fixed beam is best in both conditions: 6 μrad is best when quiet but collapses during disturbances, and 12 μrad is the reverse. The lens tracks the better state in each phase (Fig. 5). It delivers 95% more throughput than the 6 μrad beam during disturbances and 7% more than the 12 μrad beam, without giving up quiet-period capacity; overall it gains 4% over the best fixed beam.

The ideal controller changes state 80 times in 60 s, mostly between neighboring states when the jitter estimate sits near a decision boundary (Fig. 5(b)). Measured variable-focus lenses respond in about 0.2 s [12], and the prototype of [15] slews divergence at 13.6 μrad/ms, covering its full range in about 0.9 s. We therefore add an actuation latency between the decision and the lens reaching the new state; the rate is still chosen for the commanded state, so a lagging lens causes

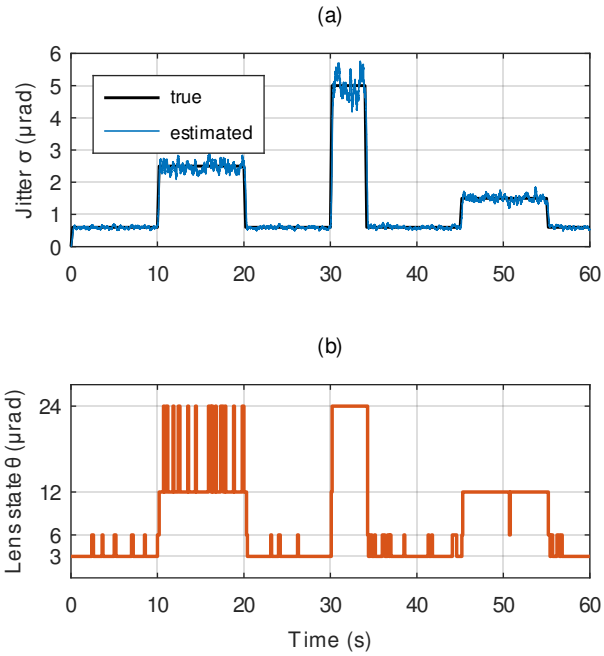

Fig. 5. 60 s LEO–GEO episode. (a) True and estimated per-axis jitter. (b) Lens state selected by the controller.

TABLE VII
EFFECT OF LENS ACTUATION LATENCY ON THE ADAPTIVE TERMINAL

Latency	Throughput (Mb/s)		
(s)	Quiet	Disturbed	Overall
0	9,850	1,357	6,431
0.05	9,827	1,354	6,417
0.1	9,804	1,352	6,402
0.2	9,721	1,344	6,349
0.5	9,471	1,331	6,194
1.0	9,053	1,331	5,944

real losses. Table VII shows that the disturbed-period gain is robust: at 0.5 s latency the lens still delivers 1,331 Mb/s against 694 Mb/s for the best quiet-period beam. The overall advantage, however, is lost at 1 s, when slow return to narrow states erodes quiet-period throughput below that of the fixed 6 μrad beam (6,160 Mb/s).

VI. DISCUSSION

Three design rules follow.

1) *Specify sensitivity in photons per bit.* About 41 photons/bit uncoded, or 16.5 per information bit with 7% HD-FEC, is realistic for pre-amplified DPSK with the losses assumed here. A flat -55 dBm requirement over 50 Mb/s–10 Gb/s is unachievable with binary DPSK or OOK.
2) *Fixed-rate inter-satellite links do not need adaptive divergence.* Set the beam so that the peak received power is e times the sensitivity; jitter then only sets the achievable outage.
3) *Adapt the divergence when the rate adapts or when the link crosses the atmosphere.* The gain concentrates

in disturbance episodes, a few lens states suffice, and actuation latencies up to about 0.5 s are tolerable.

The study has limitations. The far-field model assumes a receive aperture much smaller than the beam footprint and ignores aperture averaging. Jitter is zero-mean; boresight bias is not modeled. OOK uses the Gaussian approximation, and DPSK uses an analytic model with a fixed implementation penalty. Turbulence strengths are representative rather than derived from an altitude profile at a given elevation. The lens is modeled as ideal apart from latency, with no wavefront error, insertion loss or thermal drift, and its space qualification is preliminary [14]. The controller has no hysteresis; adding hysteresis would reduce the 80 state changes and is likely to improve the latency tolerance.

VII. Conclusion

For binary 1550 nm receivers, a -55 dBm requirement can be met only up to 595 Mb/s with practical pre-amplified DPSK, 1.5 Gb/s with 7% HD-FEC, and 4.7 Gb/s even for an ideal receiver with that FEC; at 10 Gb/s it is out of reach. Whether adaptive divergence pays off depends on the operating mode. For a fixed-rate link under pointing jitter alone, the outage-optimal divergence is independent of jitter and places the peak power at e times the sensitivity. For a rate-adaptive link it scales as $\sigma\sqrt{-4\ln P_{\mathrm{out}}}$, and turbulence makes it jitter-dependent even at a fixed rate. A four-state liquid lens recovers 95% more throughput than the best fixed beam during disturbances and keeps its overall advantage for latencies up to 0.5 s. Future work includes soft-decision FEC and coherent receivers, measured reaction-wheel jitter spectra, hysteresis in the controller, and a laboratory demonstration with a liquid lens, a piezoelectric jitter source and a 1 Gb/s DPSK link.

Data Availability

The MATLAB code that generates every figure and table in this paper is available from the author on request.

Acknowledgment

The author used Claude (Anthropic), an AI assistant, to help develop the simulation code and draft the manuscript text. All results were produced by the author's simulation code, and the author reviewed the content and takes full responsibility for it.

References

[1] K. Böhmer, M. Gregory, F. Heine, H. Kämpfner, R. Lange, M. Lutzer, and R. Meyer, "Laser communication terminals for the European Data Relay System," in *Proc. SPIE*, vol. 8246, 2012, Art. no. 82460D, doi: 10.1117/12.906798.

[2] H. Kaushal and G. Kaddoum, "Optical communication in space: Challenges and mitigation techniques," *IEEE Commun. Surveys Tuts.*, vol. 19, no. 1, pp. 57–96, 2017, doi: 10.1109/COMST.2016.2603518.

[3] Indian Space Research Organisation, "RESPOND Basket 2025," problem RES-SAC-2025-007, Dec. 2025. [Online]. Available: https://www.isro.gov.in/RESPOND_BASKET_2025.html

[4] D. O. Caplan, "Laser communication transmitter and receiver design," *J. Opt. Fiber Commun. Rep.*, vol. 4, pp. 225–362, 2007, doi: 10.1007/s10297-006-0079-z.

[5] C.-C. Chen and C. S. Gardner, "Impact of random pointing and tracking errors on the design of coherent and incoherent optical intersatellite communication links," *IEEE Trans. Commun.*, vol. 37, no. 3, pp. 252–260, Mar. 1989, doi: 10.1109/26.20099.

[6] S. Arnon, S. Rotman, and N. S. Kopeika, "Optimum transmitter optics aperture for satellite optical communication," *IEEE Trans. Aerosp. Electron. Syst.*, vol. 34, no. 2, pp. 590–596, Apr. 1998, doi: 10.1109/7.670339.

[7] M. Toyoshima, T. Jono, K. Nakagawa, and A. Yamamoto, "Optimum divergence angle of a Gaussian beam wave in the presence of random jitter in free-space laser communication systems," *J. Opt. Soc. Amer. A*, vol. 19, no. 3, pp. 567–571, Mar. 2002, doi: 10.1364/JOSAA.19.000567.

[8] A. A. Farid and S. Hranilovic, "Outage capacity optimization for free-space optical links with pointing errors," *J. Lightw. Technol.*, vol. 25, no. 7, pp. 1702–1710, Jul. 2007, doi: 10.1109/JLT.2007.899174.

[9] S. Arnon *et al.*, "Performance limitation of laser satellite communication due to vibrations and atmospheric turbulence: Down-link scenario," *Int. J. Satell. Commun. Netw.*, vol. 21, no. 6, pp. 561–573, 2003, doi: 10.1002/sat.769.

[10] Z. Xue, B. Qi, G. Ren, and Z. Xie, "Design of optimum beam divergence angle for intersatellite optical communication systems with pointing errors," *Laser Optoelectron. Prog.*, vol. 52, no. 7, Art. no. 070602, 2015.

[11] S. Arnon, "Possible solutions to mitigate vibration effects in laser inter satellite links," in *Proc. SPIE*, vol. 4489, 2002, pp. 202–207, doi: 10.1117/12.453230.

[12] V. V. Mai and H. Kim, "Beaconless PAT and adaptive beam control using variable focus lens for free-space optical communication systems," *APL Photon.*, vol. 6, no. 2, Art. no. 020801, 2021, doi: 10.1063/5.0039108.

[13] K. Lee, V. Mai, and H. Kim, "Dynamic adaptive beam control system using variable focus lenses for laser inter-satellite link," *IEEE Photon. J.*, vol. 14, no. 4, 2022, doi: 10.1109/JPHOT.2022.3183999.

[14] F. A. Fogle, "Liquid lens beam steering and environmental testing for the miniature optical steered antenna for inter-satellite communication," S.M. thesis, Dept. Aeronaut. Astronaut., Massachusetts Inst. Technol., Cambridge, MA, USA, 2020. [Online]. Available: https://hdl.handle.net/1721.1/127076

[15] A. Carrasco-Casado *et al.*, "Prototype development and validation of a beam-divergence control system for free-space laser communications," *Front. Phys.*, vol. 10, Art. no. 878488, 2022, doi: 10.3389/fphy.2022.878488.

[16] F. Ahmad, S. Ramachandrapura, J. Manattayil, and V. Raghunathan, "Path-loss optimized indoor laser-based visible light communication system for variable link length gigabit-class communication," *IEEE Photon. J.*, vol. 12, no. 4, 2020.

[17] F. Ahmad, R. N. Sathisha, K. M. Jyothsna, and V. Raghunathan, "Design of variable link length indoor visible light communication system using focus tunable liquid lens," in *Proc. SPIE*, vol. 11711, 2021, pp. 96–102.

[18] R. N. Sathisha, F. Ahmad, and V. Raghunathan, "Two-user NOMA based indoor optical wireless communication with variable cell coverage using beam divergence control," in *Proc. Nat. Conf. Commun. (NCC)*, 2024, doi: 10.1109/NCC60321.2024.10485774.

[19] R. J. McIntyre, "Multiplication noise in uniform avalanche diodes," *IEEE Trans. Electron Devices*, vol. ED-13, no. 1, pp. 164–168, Jan. 1966.

[20] N. A. Olsson, "Lightwave systems with optical amplifiers," *J. Lightw. Technol.*, vol. 7, no. 7, pp. 1071–1082, Jul. 1989.

[21] *Forward Error Correction for High Bit-Rate DWDM Submarine Systems*, ITU-T Recommendation G.975.1, 2004.

[22] M. Toyoshima, Y. Takayama, H. Kunimori, T. Jono, and S. Yamakawa, "In-orbit measurements of spacecraft microvibrations for satellite laser communication links," *Opt. Eng.*, vol. 49, no. 8, Art. no. 083604, 2010.

[23] M. A. Al-Habash, L. C. Andrews, and R. L. Phillips, "Mathematical model for the irradiance probability density function of a laser beam propagating through turbulent media," *Opt. Eng.*, vol. 40, no. 8, pp. 1554–1562, Aug. 2001, doi: 10.1117/1.1386641.